HTML ABSTRACT + LINKS

Monte Carlo versus molecular dynamics simulations in heterogeneous systems: An application to the *n*-pentane liquid-vapor interface

Florent Goujon and Patrice Malfreyt[a)]
Laboratoire de Thermodynamique des Solutions et des Polymères, UMR CNRS 6003, Université Blaise Pascal, 63177 Aubiere Cedex, France

Jean-Marc Simon
Laboratoire de Recherches sur la Réactivité des Solides, UMR CNRS 5613, Université de Bourgogne, BP 47870, 21078 Dijon Cedex, France

Anne Boutin, Bernard Rousseau, and Alain H. Fuchs
Laboratoire de Chimie Physique, UMR CNRS 8000, Université Paris-Sud, 91405 Orsay, France

(Received 2 March 2004; accepted 27 September 2004)

The Monte Carlo (MC) and molecular dynamics (MD) methodologies are now well established for computing equilibrium properties in homogeneous fluids. This is not yet the case for the direct simulation of two-phase systems, which exhibit nonuniformity of the density distribution across the interface. We have performed direct MC and MD simulations of the liquid-gas interface of *n*-pentane using a standard force-field model. We obtained density and pressure components profiles along the direction normal to the interface that can be very different, depending on the truncation and long range correction strategies. We discuss the influence on predicted properties of different potential truncation schemes implemented in both MC and MD simulations. We show that the MD and MC profiles can be made in agreement by using a Lennard-Jones potential truncated via a polynomial function that makes the first and second derivatives of the potential continuous at the cutoff distance. In this case however, the predicted thermodynamic properties (phase envelope, surface tension) deviate from experiments, because of the changes made in the potential. A further readjustment of the potential parameters is needed if one wants to use this method. We conclude that a straightforward use of bulk phase force fields in MD simulations may lead to some physical inconsistencies when computing interfacial properties. © *2004 American Institute of Physics.* [DOI: 10.1063/1.1819868]

I. INTRODUCTION

Most of the phenomena in surface science (adhesion, wetting, and lubrication) involve the combination of liquid-liquid, liquid-vapor, and liquid-solid interfaces. Many important fundamental problems in chemistry and biology lead to practical applications in ion separation and extraction, drug delivery, oil recovery, and detergents. They involve ion and charge transfers, adsorption and solvation processes that occur at the vicinity of the liquid-gas interface or between two immiscible liquids. These liquid-liquid interfaces are characterized by specific electrical, structural, and dynamical properties. Due to the difficulties of experimental probes to access the molecular level structure of the interface, direct molecular simulation methods have become powerful techniques to examine the nature of the interface region and to calculate interfacial properties such as the interfacial tension and the interface thickness.

The necessity for the direct molecular simulations to provide reliable properties compared to experiments implies to simulate realistic molecular systems with appropriate energetic descriptions. Molecular simulation technique has been widely used to study the liquid-liquid interfacial properties, the energetic and the mass transfer process. However, the modeling of an oil-water interface often leads to an important difference in polarity between the two phases resulting thus in low mutual solubilities. The interface region can be thus characterized by a high density gradient and a strong asymmetry in the intermolecular interactions. These particularities make the results very sensitive to the nonbonded interaction potential models.

Wipff and co-workers[1,2] have performed molecular dynamics (MD) simulations on the oil-water interface to study the extraction of alkali cations and trivalent lanthanide cations from water to oil phases. The nonbonded interactions are described by a 6–12 pairwise contribution and the electrostatic long range interactions are calculated either using a slightly modified version of the Ewald summation technique or the reaction field method. Recent MD simulations[3] on the water-*n*-alkanes liquid-liquid interfaces show an excellent agreement between the calculated and experimental surface tension when both electrostatic interactions are handled by the Ewald summation method and two specific contributions from the real and reciprocal space are added in the surface tension calculation. MD simulations[4,5] have been applied successfully to calculate the ion transfer free energy profile across a liquid-liquid interface. This study shows the importance in including explicitly polarization effects into poten-

[a)]Author to whom correspondence should be addressed. Electronic mail: Patrice.MALFREYT@univ-bpclermont.fr

 © 2004 American Institute of Physics

Downloaded 04 Jul 2008 to 194.214.132.32. Redistribution subject to AIP license or copyright; see http://jcp.aip.org/jcp/copyright.jsp

tial model to make the results closer to the experimental interpretations of the ion transfer mechanism, especially when the two phases differ considerably in polarity. Molecular simulations reported in the literature show that the MD method has been widely applied to liquid-liquid interfaces. We also observe a great variety of methodologies used in the treatment of the repulsion-dispersion potential and long range electrostatic interactions. As a result, it is very difficult to evaluate the influence of each long range interaction potential model on the interfacial properties.

As concerns the liquid-vapor interface, numerous simulations using both direct Monte Carlo (MC) and MD methods have been undertaken. In the literature, there have been an important number of direct simulations of the liquid-vapor interface of a Lennard-Jones fluid[6–16] but this technique has not been widely applied to molecular systems.[17–21] Recently, MD simulations[22] of the liquid-vapor interface of a molten salt show that a better agreement between experimental and calculated surface tension values can be found when a full Ewald summation of dispersion interactions and polarization effects are included into the interaction model. These results corroborate what was already observed in a previous study[4,5] in the case of a liquid-liquid interface.

Since alkanes are the basis of the petrochemical industry, the determination of their phase behavior is of a great importance in many technological applications, such as for oil recovery and separation process. For this reason, there have been significant theoretical efforts towards the molecular simulation method and the potential models used for alkanes. In the united atom (UA) model, all CH_3 and CH_2 are treated as neutral interaction sites and the repulsion-dispersion interaction between these sites are only described by means of a Lennard-Jones (LJ) 6–12 potential.

We have shown in previous papers[23,24] that the direct MC method of simulating liquid-vapor interface of *n*-alkanes is now well established. The key feature in these systems is the nonuniformity of the density distribution along the direction normal to the interface. This implies that the usual treatments for homogeneous systems may not be applied any longer. The long range corrections to the configurational energy to the pressure components and to the interfacial tension must be carefully applied with the use of truncated potential and forces. We have used the local long range corrections to the configurational energy developed by Guo and Lu[25] within the Metropolis scheme and we have demonstrated that we obtain the thermal equilibrium conditions by calculating the profiles of the configurational temperature along the direction normal to the surface. The equality between the normal and tangential pressures throughout the liquid and vapor phases has been highlighted once two contributions of the long range corrections to the pressure tensor components were included. The coexisting densities and the critical points were in good agreement with the experimental results. We have also calculated the long range corrections to the surface tension using different analytical forms and we have shown that this tail contribution may represent up to 30% of the total value. We have also checked that the dependence of the surface tension with system size and the cutoff radius was cancelled as the long range corrections were taken into account. However, recent works[26,27] have shown that it was also possible to avoid the inclusion of long range corrections by using the lattice sum method for the dispersion term of the Lennard-Jones potential.

One of the objectives of this work is to calculate the residence time of alkane molecules at the liquid-vapor interface region. This important dynamical property can only be calculated from MD. Before doing this, it is interesting to determine the coexistence curve of an alkane using MD technique, especially as the force field parameters used in MD have been preliminary established from MC calculations. This comparison leads to a quantitative evaluation of the differences between MC and MD on the coexisting densities, critical properties, and interfacial properties.

In principle, these two methods should lead to the same equilibrium properties although they differ in the way of generating the trajectory in the phase space. MC simulation aims to explore the configurational space of a system using the calculation of changes in intermolecular energy whereas MD simulation generates configurations by solving the classical equations of motions using the forces. The differences between MC and MD techniques on inhomogeneous systems have been highlighted for a long time. It was already shown that MC and MD methods yield different coexisting densities in the case of the liquid-vapor coexistence curve of Lennard-Jones fluids.[14] These differences between MC and MD results are explained by the fact that the potential in MC is not differentiable at the cutoff value and that consequently the force used in MD does not correspond to the potential in MC. MC and MD are therefore carried out with different potential models. Making MC and MD consistent requires an investigation on the conditions of the differentiability of the potential function and amounts to address the question of the discontinuity of the potential at the cutoff value. In fact, differentiating a truncated potential with respect to r gives a δ function at the cutoff value, which consequently causes impulses on an atom pair whose separation distance crosses the cutoff. This delta function is not considered as crucial in the simulations of a homogeneous fluid because we may assume that the forces affecting a particle from outside its cutoff sphere will average out. This explains why no significant differences are usually observed between MC and MD simulations for homogeneous systems. In the case of inhomogeneous system, this assumption is no longer valid.

To solve this problem, Trokhymchuk and Alejandre[13] have added a δ function to the force taking thus into account the discontinuous change in the potential at the cut off. They have performed direct simulations of the liquid-vapor interface of a Lennard-Jones fluid and have shown that including this δ function in MD simulations makes the coexistence properties (densities, normal and tangential pressures and surface tension) identical to those calculated in MC simulations with a truncated potential.

We have reinvestigated the conditions under which MC and MD yield similar results concerning the coexistence properties and the thermodynamic equilibria on a molecular system. To do this, we perform MD simulations using different analytical forms for the force (truncated, truncated, and shifted, truncated LJ modified by a cubic spline) and MC

Downloaded 04 Jul 2008 to 194.214.132.32. Redistribution subject to AIP license or copyright; see http://jcp.aip.org/jcp/copyright.jsp

simulations with the corresponding potential. We will be comparing the MC and MD methods on a molecular system with a vapor-liquid density coexistence curve and surface tension values already established by experiments and by different molecular simulations methods MC (Refs. 23 and 24) and GEMC (Ref. 28). The coexisting densities, the surface tension, and its long range corrections, the normal and tangential pressure components are calculated as a function of the expressions of the potentials and forces used.

We check what it was already observed on the Lennard-Jones fluid liquid-vapor interface. The coexisting densities calculated from MC using a truncated potential and from MD using a truncated force are different.[13,14] The use of a shifted potential with MC decreases the discrepancy with MD. To obtain a close agreement between MC and MD, we have chosen to remove discontinuities in the energy and force equations by modifying the LJ potential via an additional polynomial function.

This paper is organized as follows: In Sec. II, we describe the intramolecular and intermolecular potentials used in the MC and MD simulations. In Sec. III, we detail the setup of the MC and MD simulations and we give the different expressions for the calculation of the pressure components for both MC and MD techniques. We present the expressions of the configurational temperature and of the long range corrections to the surface tension. Section IV compares the results from MC and MD as a function of the form of the potential used. We end up this section by the calculation of the residence time of pentane molecules in the interface region. We conclude in Sec. V, with a short summary of our main results.

II. SIMULATION METHOD

A. Interaction model

The *n*-pentane is modeled as a flexible molecule containing five united atom sites using the TraPPE (Ref. 29) alkane model. The sites i and j on different molecules and sites on the same molecule, separated by more than three bonds, interact through a Lennard-Jones potential

$$u_{LJ}(r_{ij}) = 4\epsilon_{ij}\left[\left(\frac{\sigma_{ij}}{r_{ij}}\right)^{12} - \left(\frac{\sigma_{ij}}{r_{ij}}\right)^{6}\right], \tag{1}$$

where ϵ_{ij} is the energy parameter of the interaction, σ_{ij} is the Lennard-Jones core diameter, and r_{ij} is the distance between interaction sites i and j. The LJ parameters for the interactions between sites of different types are calculated by using the Lorentz-Berthelot mixing rules:

$$\epsilon_{ij} = (\epsilon_{ii}\epsilon_{jj})^{1/2}, \quad \sigma_{ij} = \tfrac{1}{2}(\sigma_{ii} + \sigma_{jj}). \tag{2}$$

The interaction sites have the following Lennard-Jones parameters: $\epsilon_{CH_3}/k_B = 98$ K and $\epsilon_{CH_2}/k_B = 46$ K, where k_B is Boltzmann's constant. The size parameters are $\sigma_{CH_3} = 3.75$ Å and $\sigma_{CH_2} = 3.95$ Å.

The bond distance between two sites is fixed at the separation of 1.54 Å. The bond-angle interactions are harmonic, with

$$u_{bend} = \tfrac{1}{2}k_\theta(\theta - \theta_o)^2, \tag{3}$$

where θ is the angle between three consecutive united atoms, $k_\theta/k_B = 62\,500$ K rad^{-2} is the bending constant, and $\theta_o = 114°$ is the equilibrium bond angle.

In pentane, the two torsional potentials are represented by the OPLS potential model[30]

$$u_{tors} = c_1(1 + \cos\phi) + c_2(1 - \cos 2\phi) + c_3(1 + \cos 3\phi), \tag{4}$$

where ϕ is the dihedral angle between four subsequent united atoms, $c_1/k_B = 355.03$ K, $c_2/k_B = -68.19$ K, and $c_3/k_B = 791.32$ K.

B. Methodology

The simulation box is a rectangular parallelepiped box of dimensions $L_x L_y L_z$ ($L_x = L_y = 30$ Å, $L_z = 200$ Å) with $N = 300$ pentane molecules. The periodic boundary conditions are applied in the three directions. MC simulations are performed in the NVT ensemble. Each cycle consists of N randomly selected moves with fixed probabilities. The moves are (1) displacement of the center of mass of a random molecule, (2) rotation of a randomly selected molecule around its center of mass, and (3) regrowth of part of a random molecule using the configurational-bias scheme.[31] The relative probabilities for the different types of moves are 0.45 for translations, 0.35 for rotations, and 0.20 for the modification of the conformation. The maximum displacement and maximum rotation are adjusted during the equilibration phase to give an acceptance ration of 0.4. As concerns the translational moves, two different displacements have been chosen randomly with equal probability. The adjustment of these two maximum displacements, during the equilibration phase, give acceptance ratios of 20% and 60%. This specificity for the translational moves improves the sampling of the configurational space of the vapor phase. Further details concerning the specifications of the MC simulations can be found in a previous paper.[24] The MD simulations have been performed in the NVT ensemble using the Nosé-Hoover thermostat.[32] The first-order equations of motions are integrated using a five-value Gear predictor-corrector procedure with a time step Δt of 2 fs. The C–C bond lengths are constrained to a fixed distance using the Gauss's principle of least constraint.[33]

The initial configuration has been built by placing the center of mass of N *n*-pentane molecules on a cubic lattice with random orientations. MC and MD simulations in the NPT ensemble have been performed on this bulk fluid configuration. The dimension of the resulting box has been increased along the z axis by placing two empty cells on both sides of the bulk liquid box. A typical MC run consists of 50 000 cycles for equilibration and 100 000 cycles for the production phase. Equilibration in MD is performed over 200 000 steps whereas the acquisition phase is carried out over 10^6 steps. The total simulation time for the production runs is 2 ns. The configurational temperature, the normal and tangential components of the pressure tensor, the surface tension and the coexisting densities are calculated every ten cycles for the MC simulation and every 100 steps for the MD simulation. This means that, in both methods, the calculation of the thermodynamic properties is performed over 10 000

Downloaded 04 Jul 2008 to 194.214.132.32. Redistribution subject to AIP license or copyright; see http://jcp.aip.org/jcp/copyright.jsp

configurations. The statistical errors in these properties are estimated using five blocks averages of 2000 configurations. For the geometry of the system, we expect there a dependence of the thermodynamic properties only in the direction normal to the interface. We have therefore calculated the profiles of the temperature, pressure, and surface tension and its long range correction as a function of z by splitting the cell into slabs of width δz.

C. Thermal equilibrium

The configurational temperature[34–36] profile along the direction normal to the interface may be expressed as follows:

$$k_B T_{conf}(z_k) = \frac{\langle \Sigma_{i=1}^{N} H_k(z_i) \mathbf{F}_\mathbf{i}^2 \rangle}{\left\langle \Sigma_{i=1}^{N} H_k(z_i) \left(\frac{\partial F_{ix}}{\partial r_{ix}} + \frac{\partial F_{iy}}{\partial r_{iy}} + \frac{\partial F_{iz}}{\partial r_{iz}} \right) \right\rangle}, \tag{5}$$

where $\mathbf{F}_i$ is the intermolecular force on molecule i acting upon the molecular center-of-mass $\mathbf{r_i}$, and $H_k(z_i)$ is a top-hat function defined such that

$$H_k(z_i) = \begin{cases} 1 & \text{for } z_k - \frac{\delta z}{2} < z_i < z_k + \frac{\delta z}{2}. \\ 0 & \text{otherwise} \end{cases} \tag{6}$$

The configurational temperature profile can be calculated in both MC and MD simulations and can be compared in MD simulations with the temperature calculated from the molecular momenta, according to the following equation:

$$k_B T_z(z_k) = \left\langle \frac{\Sigma_{i=1}^{N} H_k(z_i) m_i (\mathbf{v_i})_z . (\mathbf{v_i})_z}{\Sigma_{i=1}^{N} H_k(z_i)} \right\rangle, \tag{7}$$

where $T_z(z_k)$ is the slab temperature in the z direction, and m_i and $(\mathbf{v_i})_z$ are the molecular mass and z component of the velocity of the center of mass of molecule i, respectively.

D. Mechanical equilibrium

In the case of an equilibrium planar interface, the Irving-Kirkwood definition (IK) (Refs. 37 and 38) of the pressure tensor leads to the following expression for the $p_{\alpha\beta}$ component as a function of z. The $p_{\alpha\beta}$ component is thus composed of an ideal gas contribution $p_{\alpha\beta}^{id}$ and a potential part $p_{\alpha\beta}^{conf}$, defined in Eqs. (8a) and (8b), respectively,

$$p_{\alpha\beta}^{id}(z_k) = \langle \rho(z_k) \rangle k_B T \mathbf{I}, \tag{8a}$$

$$p_{\alpha\beta}^{conf}(z_k) = \frac{1}{A} \left\langle \sum_{i=1}^{N-1} \sum_{j>i}^{N} (\mathbf{r_{ij}})_\alpha \times (\mathbf{F_{ij}})_\beta \frac{1}{|z_{ij}|} \theta\left(\frac{z_k - z_i}{z_{ij}} \right) \theta\left(\frac{z_j - z_k}{z_{ij}} \right) \right\rangle, \tag{8b}$$

where $\langle \cdots \rangle$ denotes a canonical ensemble average. $\rho(z_k)$ is the molecular density profile along the z direction, $\mathbf{I}$ is the unit tensor, and T is the input temperature. α and β represent x, y, or z directions. $\theta(x)$ is the unit step function defined by $\theta(x)=0$ when $x<0$ and $\theta(x)=1$ when $x \geqslant 0$. A is the surface area normal to the z axis. The distance z_{ij} between two molecular centers of mass is divided into N_s slabs of thickness $\delta z = 1.0$ Å, and the molecules i and j give a local contribution to the pressure tensor in a given slab if the line joining i and j crosses, starts or finishes in the slab. Each slab has $1/N_s$ of the total contribution from the $i-j$ interaction. The normal component $p_N(z_k)$ is equal to $p_{zz}(z_k)$ whereas the tangential component is given by $(1/2) \times [p_{xx}(z_k) + p_{yy}(z_k)]$. The ideal contribution of $p_{\alpha\beta}^{id}$ component, defined in Eq. (8a), may be compared, in MD, to the kinetic part $p_{\alpha\beta}^{kin}$ according to

$$p_{\alpha\beta}^{kin} = \frac{1}{V_s} \left\langle \sum_{i,\alpha,\beta} H_k(z_i) m_i (\mathbf{v_i})_\alpha (\mathbf{v_i})_\beta \right\rangle, \tag{9}$$

where $V_s = L_x L_y \delta z$ is thus the volume of the basic slab and $(\mathbf{v_i})_\alpha$ is the α component of the velocity of the molecular center of mass.

An alternative technique for calculating the normal component of the pressure tensor is based upon the method of planes (MOP) (Refs. 39 and 40) and expresses the $p_{\alpha z}$ component as

$$p_{\alpha z}^{kin}(z_k) = \frac{1}{A} \left\langle \sum_{i=1}^{N} m_i (\mathbf{v_i})_\alpha \frac{1}{\Delta t} \mathrm{sgn}[(\mathbf{v_i})_z] \right\rangle, \tag{10a}$$

$$p_{\alpha z}^{conf}(z_k) = \frac{1}{A} \sum_{i=1}^{N-1} \sum_{j>i}^{N} (\mathbf{F_{ij}})_\alpha [\theta(z_i - z_k)\theta(z_k - z_j) - \theta(z_j - z_k)\theta(z_k - z_i)], \tag{10b}$$

where Eqs. (10a) and (10b) represent a z component of the kinetic $p_{\alpha z}^{kin}(z_k)$ and potential $p_{\alpha z}^{conf}(z_k)$ parts, respectively. The kinetic part is due to the momentum carried out by the molecules as they cross the area during Δt. If between time t and $t+\Delta t$, atom i moves through planes, we use the sign of the z component of the velocity to specify the direction of the crossing. In all cases, the contribution to the pressure tensor will be positive. As concerns the configurational part, the first product of the Heaviside is zero and the second product is unity, if the following conditions $(z_i < z_k)$ and $(z_j > z_k)$ are satisfied. If $(z_i > z_k)$ and $(z_j < z_k)$, the first product is unity and the second one is zero. The contribution to the pressure tensor is zero if both z_i and z_j are either smaller or larger than z_k.

E. Surface tension

The calculation of the molecular surface tension[41] for the system with two planar interfaces is given by

$$\gamma = \frac{1}{2A} \left\langle \sum_{i=1}^{N-1} \sum_{j=i+1}^{N} \sum_{a=1}^{5} \sum_{b=1}^{5} \times \frac{\mathbf{r_{ij}} . \mathbf{r_{iajb}} - 3 z_{ij} z_{iajb}}{2 r_{iajb}} \frac{du_{LJ}(r_{iajb})}{dr_{iajb}} \right\rangle. \tag{11}$$

The integration of the difference between the profiles of the normal and tangential parts of the pressure tensor represents an alternative way for the calculation of the surface tension. We have already shown that these two definitions lead to the same results for the surface tension within statis-

Downloaded 04 Jul 2008 to 194.214.132.32. Redistribution subject to AIP license or copyright; see http://jcp.aip.org/jcp/copyright.jsp

tical uncertainty.[24] We have also shown that the calculation of the surface tension is very sensitive to the cutoff value and necessitates the addition of long range corrections. Various analytical forms[24] have been compared and the following form[25] is used throughout this work to determine a profile along the direction normal to the interface.

$$\gamma_{(lrc)}(z_k)=\frac{\pi}{2}\rho(z_k)\frac{V_s}{A}\int_{r_c}^{\infty}dr\int_{-r}^{r}d\Delta z\sum_{i=1}^{n_z}[\rho(z_i)-\rho(z_{i-1})]\frac{du_{LJ,m}}{dr}[r^2-3(\Delta z)^2], \quad (12)$$

where Δz is equal to the difference $z-z_k$, $u_{LJ,m}$ is the intermolecular energy between two pentane molecules, and r is the difference between the two centers of mass. The total long range correction is calculated by summing up all the contributions to the local values of each slab and dividing the result by 2.

III. RESULTS AND DISCUSSIONS

A. MC and MD with truncated models

The aim of this section is to quantify the inconsistencies of the coexisting densities, critical temperature, and surface tensions along the coexistence curve of the *n*-pentane between the MC method using a truncated potential and the MD using a truncated force. We are using here for a polyatomic-heterogeneous molecular system the methods previously used for studying a simple LJ system.

Herein, we use a relatively small cutoff ($r_c=12$ Å) to maintain an objective of computational efficiency. As concerns the algorithmic specificities of the MC code, we use a truncated potential u_{LJ} in which we include long range contributions. The long range corrections to the total energy is composed of two terms;[25] the first term depends on the local density and the second one takes into consideration that each slab is surrounded with neighboring slabs with different densities. We have also shown[24] that the calculation of the second part is very cumbersome and that the fact of neglecting this term amounts to overestimate the long range correction of 13%. For computational efficiency, only the first part is considered. The long range correction is then calculated at every change in the position of a molecular center of mass, occurring during the translational and internal configurational moves. This tail correction is obtained by summing up the corresponding local contributions and then implemented in the acceptance rule. For the MD simulations, we use only a truncated and unshifted force and no long range correction is added to the force.

We compare the results for MC and MD at four different temperatures (299 K, 325 K, 350 K, and 375 K). The coexisting densities result from the fit to the molecular density profiles using Eq. (13)

$$\rho(z_k)=\frac{1}{2}(\rho_l+\rho_v)-\frac{1}{2}(\rho_l-\rho_v)\tanh\left[\frac{2(z_k-z_o)}{d}\right], \quad (13)$$

where ρ_l and ρ_v are the coexisting densities of the liquid and vapor phases, respectively. z_o indicates the position of the Gibbs surface and d represents the interfacial thickness. Figure 1(a) shows the coexisting densities calculated from MC and MD simulations. As should be expected from a force field[29] established from MC simulations, we check in Fig. 1(a) that the phase envelope is better predicted using MC calculations than using MD. We note that the incorporation of the long range corrections into the truncated potential in MC improves the agreement with experiments. However, the magnitude of the differences observed between MC and MD is too important to be explained by only the presence of these long range corrections. In fact, deviations of the liquid and vapor densities from experimental values increases from

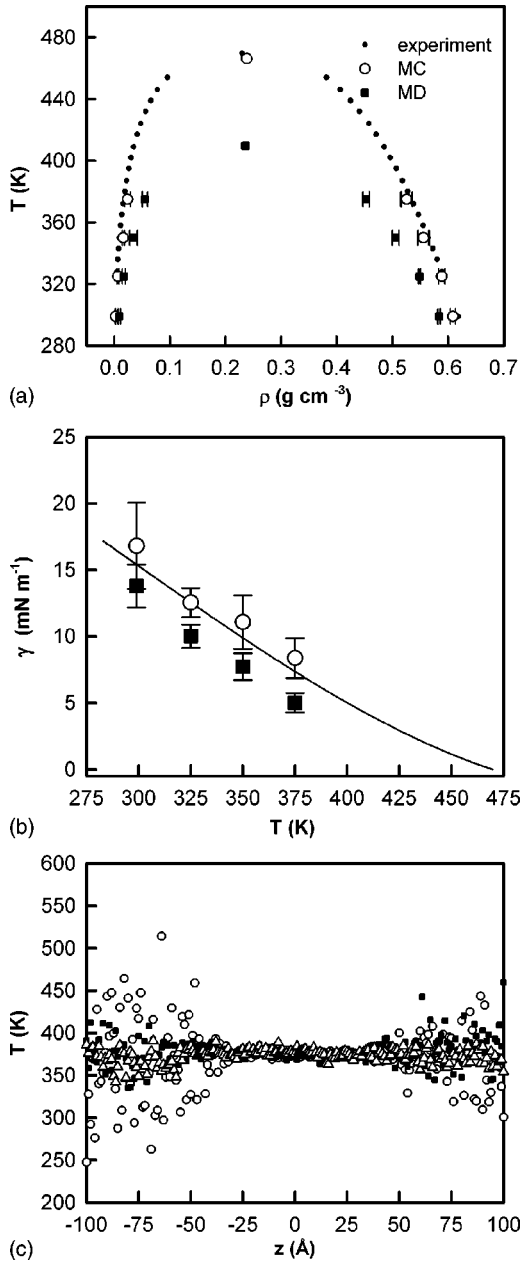

FIG. 1. (a) Vapor-liquid coexistence curve of *n*-pentane computed from MC and MD simulations and compared with experimental data[42] (●); (b) calculated surface tension as a function of the temperature in both MC and MD. The solid line represents the experimental values;[42] (c) configurational temperature profiles calculated in MC and MD. The temperature profile represented by (△) is calculated from Eq. (7). In parts (a), (b), and (c), the equilibrium properties calculated in MC and MD are represented by (○) and (■), respectively.

Downloaded 04 Jul 2008 to 194.214.132.32. Redistribution subject to AIP license or copyright; see http://jcp.aip.org/jcp/copyright.jsp

TABLE I. Simulation results for *n*-pentane using MC and MD calculations. The vapor density (ρ_l) and liquid density (ρ_l) are given in g cm^{-3}. The total surface tension γ_{tot}, represents the sum of the (γ) part calculated from Eq. (11) and of the long range correction contribution defined in Eq. (12). All the surface tension values are reported in mN m^{-1}. The subscript indicates the accuracy of the last decimal (s). The number 0.556_{10} means 0.556 ± 0.010.

T/K	ρ_l	ρ_v	γ_{lrc}	γ	γ_{tot}
		MC			
299	0.609_5	$0.000\,23_2$	5.5_1	11.3_{35}	16.8_{35}
325	0.589_6	$0.000\,65_{15}$	4.8_1	7.7_{10}	12.5_{11}
350	0.556_{10}	0.016_2	4.1_1	6.9_{20}	11.0_{10}
375	0.526_{10}	0.024_5	3.2_1	5.1_8	8.3_8
		MD			
299	0.584_2	0.009_2	4.7_1	9.1_{16}	13.8_{16}
325	0.549_2	0.017_3	3.8_1	6.2_8	10.0_9
350	0.506_6	0.035_7	3.0_1	4.7_9	7.7_{10}
375	0.453_6	0.055_5	2.1_1	2.9_1	5.0_7

1.8% for MC to 11% for MD. The estimate of the critical point has been carried out by fitting the calculated coexistence density to the scaling law for the density and law of rectilinear diameters, using an Ising-type critical exponent of $\beta = 0.32$. The critical temperature T_c is $= 466.1$ K and 409.7 K, using MC and MD calculations, respectively. The critical density ρ_c is 0.238 for MC and 0.236 for MD. T_c is predicted within 1% using MC and 13% using MD whereas ρ_c is predicted within 4% for both methods. We see that, at a given T, the liquid densities calculated using MD are smaller than those calculated using MC and that the vapor densities from MD are greater than those from MC. It means that the phase diagram calculated using MD is shifted vertically to the low temperatures, leading thus to an important deviation for T_c compared to the experimental value. We expect, thus, the surface tension values calculated from MD to be smaller than those calculated from MC. Figure 1(b) confirms this point of view with deviations from experimental surface tension values within 7.5% for MC and 24% for MD. We also observe that the long range corrections to the surface tension can represent up to 38% of the total value (Table I). We check that the long range corrections calculated in MD are smaller than those in MC and follow the same trend as the contribution resulting from the virial expression using Eq. (11).

Figure 1(c) shows the profiles of the configurational temperature calculated in MC and MD with that of the temperature calculated from the momenta according to Eq. (7) at $T = 375$ K. We check that the profiles may be considered as constant within the fluctuations in both the liquid and vapor phases and correspond to the input temperature. The temperature calculated from averages over the slabs in the vapor phases is $= 376 \pm 21$ K and 368 ± 60 K for MD and MC, respectively. The average temperature calculated in the liquid phase is 376 ± 5 K for MD and 375 ± 3 K for MC. Temperature fluctuations in the vapor phase are more important for MC than for MD. This may be explained by the fact that the vapor density calculated in MC is smaller than that resulting from MD. For MD, the statistics in the vapor phase is therefore improved due to a larger number of molecules per slab. The average temperature calculated in MD from the momenta matches also very well with the input temperature ($T_{vap} = 370 \pm 12$ K and $T_{liq} = 377 \pm 5$ K). We also check that the diagonal elements T_{xx} and T_{yy} are equivalent to T_{zz} within the fluctuations showing thus an equipartition of the kinetic energy in the three directions. The profiles of the off-diagonal elements of the temperature tensor fluctuate about a zero mean value, as expected for a system at thermal equilibrium. From the temperature profiles, we check that both MC and MD correctly sample the canonical ensemble and that the difference in coexisting densities and surface tensions between MC and MD are not due to shifts in the calculated temperature. Moreover, we check that thermal equilibrium of the liquid-vapor interface is obtained in both MC and MD.

From MC and MD simulations, we can draw the following conclusions: first, the MC calculations using the first part of the long range corrections to the configurational energy with a truncated potential and a relatively small cutoff yield coexisting densities and surface tensions in close agreement with the corresponding experimental values. This result is consistent with the fact that the set of LJ parameters of the force field has been developed from MC calculations. Second, the phase diagram of the *n*-pentane calculated from the MD method with a truncated force is shifted to the low temperatures. This particularity is in line with what it was observed in previous simulations of the liquid-vapor coexistence curve of LJ fluids.[13,14] The fact that the potential function is not differentiable at the cutoff value makes the MC and MD calculations different. Moreover, the differences are slightly increased by the fact that MC uses a potential modified by the presence of long range corrections. Consequently, in what follows, we try to evaluate the importance of the truncation procedures on different potential functions and to analyze the magnitude of the discrepancies between MC and MD when the potential and force equations change accordingly.

B. MC and MD with truncated and shifted models

We compare, in Fig. 2(a), the density profiles calculated both from MC using a truncated u_T potential usind Eq. (14) without any long range corrections applied to the potential and from MD using a truncated f_T force according to Eq. (16). We also add for comparison the density profiles resulting from MC using the truncated potential, corrected by long range corrections to the configurational energy and from MC using a truncated and shifted u_{TS1} potential defined in Eq. (15). We check in Fig. 2(a) and in Table II that the incorporation of long range corrections to the total energy increases the liquid density and decreases the vapor density leading thus to surface tension slightly larger and closer to the experimental value. This particularity, already observed in a previous work,[23] confirms that a better prediction of the coexistence properties is observed when the long range corrections are included in the Metropolis scheme. Second, MC calculations with the u_{TS1} model, where a constant term is

Downloaded 04 Jul 2008 to 194.214.132.32. Redistribution subject to AIP license or copyright; see http://jcp.aip.org/jcp/copyright.jsp

TABLE II. Simulation results for *n*-pentane using MC and MD calculations with different analytical shapes for the potential energy and the force at $T=325$ K. The vapor density ρ_l and liquid density ρ_l are expressed in g cm^{-3}. The total surface tension γ_{tot}, the γ part and its long range corrections are reported in mN m^{-1}. The experimental data result from Dortmund Data Bank.[42] The subscript indicates the accuracy of the last decimal (s). The number 0.589_6 means 0.589 ± 0.006.

	ρ_l	ρ_v	γ_{lrc}	γ	γ_{tot}
Expt. T=328 K	0.589	0.0052			12.3
MC $u_T+\Sigma u_{lrc}$	0.589_6	0.0065_{15}	4.8_1	7.7_{10}	12.5_{10}
MC u_T	0.578_1	0.008_1	4.6_1	7.3_{18}	11.9_{18}
MC u_{TS1}	0.559_1	0.019_2	4.1_1	7.6_{11}	11.7_{11}
MC u_{TS2}	0.520_1	0.029_1	0	3.4_{16}	3.4_{16}
MC u_{SP}	0.541_1	0.021_1	0	6.2_{17}	6.2_{17}
MD f_T	0.549_2	0.017_3	3.8_1	6.2_8	10.0_9
MD f_{TS}	0.511_1	0.030_1	0	3.2_7	3.2_7
MD (f_{SP}, $r_c=12$ Å)	0.541_1	0.021_2	0	5.0_{13}	5.0_{13}
MD (f_{SP}, $r_c=15$ Å)	0.567_2	0.011_1	0	8.0_{17}	8.0_{17}

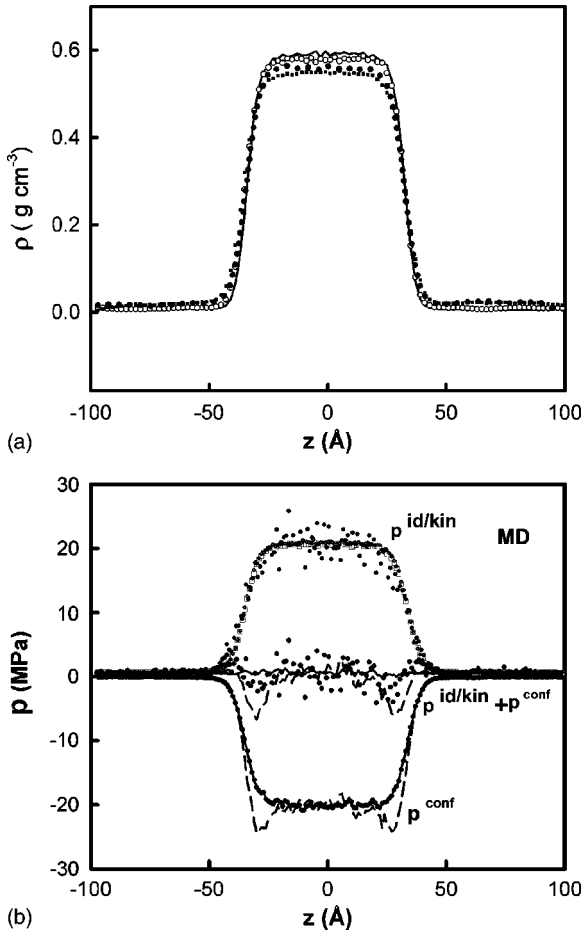

FIG. 2. (a) Density profiles calculated at $T=325$ K from different truncation procedures and methods. MC, $u_T+\Sigma u_{lrc}$, (——); MC, u_T, (○); MC, u_{TS1}, (●); MD, f_T, (■); (b) normal (——) and tangential (— — —) pressure profiles calculated from the IK method in MD using a truncated force. (●) normal components (kinetic, potential, and total parts) calculated from the method of planes. $p^{id/kin}$ and p^{conf} indicate the different contributions; the ideal gas contribution is represented by (□) and the kinetic part by (○). The curves in the center of the part (b) correspond to the total pressure expressed as the sum of the ideal and potential parts.

subtracted from the potential at all the values, underestimates the liquid density and overestimates the vapor density compared to simulations with unshifted potential. As a consequence, the effect of shifting potential should lower the critical point as it was already observed for the determination of phase diagrams of LJ fluids using GEMC method.[43,44] The MD simulation using the f_T force yields a density profile different from the MC simulations using u_T. When the MC simulation is carried out with u_{TS1}, the agreement with MD using f_T is improved.

$$u_T(r_{ij})=\begin{cases} u_{LJ}(r_{ij}) & r_{ij}<r_c \\ 0 & r_{ij}\geqslant r_c \end{cases}, \tag{14}$$

$$u_{TS1}(r_{ij})=\begin{cases} u_{LJ}(r_{ij})-u_{LJ}(r_c) & r_{ij}<r_c \\ 0 & r_{ij}\geqslant r_c \end{cases}, \tag{15}$$

$$f_T(r_{ij})=\begin{cases} -\dfrac{\partial u_{LJ}}{\partial r_{ij}} & r_{ij}<r_c \\ 0 & r_{ij}\geqslant r_c \end{cases}. \tag{16}$$

The study of the components of the pressure tensor is very instructive. As concerns the pressure profiles computed from MD simulations [Fig. 2(b)], we check that the profiles of the ideal p_{zz}^{id} and kinetic p_{zz}^{kin} components are equivalent and superimposed in Fig. 2(b) and cannot be distinguished on the scale of the figure. The kinetic part profile calculated from the momentum flux using the method of planes presents local values located on both sides of the profile of the ideal part. The kinetic part calculated both from the Irving-Kirkwood and MOP definitions are shown to be similar within the statistical uncertainties with a noisier profile for the MOP method. The profiles of the potential part of p_{zz} component calculated from these two methods are very close, as it was already shown for MC calculations.[24] The normal pressure is constant throughout the simulation box. The tangential pressure has also the same value in the liquid and vapor phases and is equal to the normal pressure away from interface regions. The tangential pressure presents two negative peaks at the interfaces showing that the liquid phase is under compression. We also note that the configurations calculated from MD with the f_T force are in mechanical equilibrium, as expected from a method which uses directly the forces to generate the evolution of the system. It means that the profiles of the pressure components need not be corrected by the addition of long range corrections to obtain mechanical equilibrium. On the other hand, these corrections were required to demonstrate the mechanical equilibrium in the case of MC simulations using a truncated potential with its long range corrections incorporated in the Metropolis scheme.[24]

Figure 3(a) displays the profiles of the tangential and

Downloaded 04 Jul 2008 to 194.214.132.32. Redistribution subject to AIP license or copyright; see http://jcp.aip.org/jcp/copyright.jsp

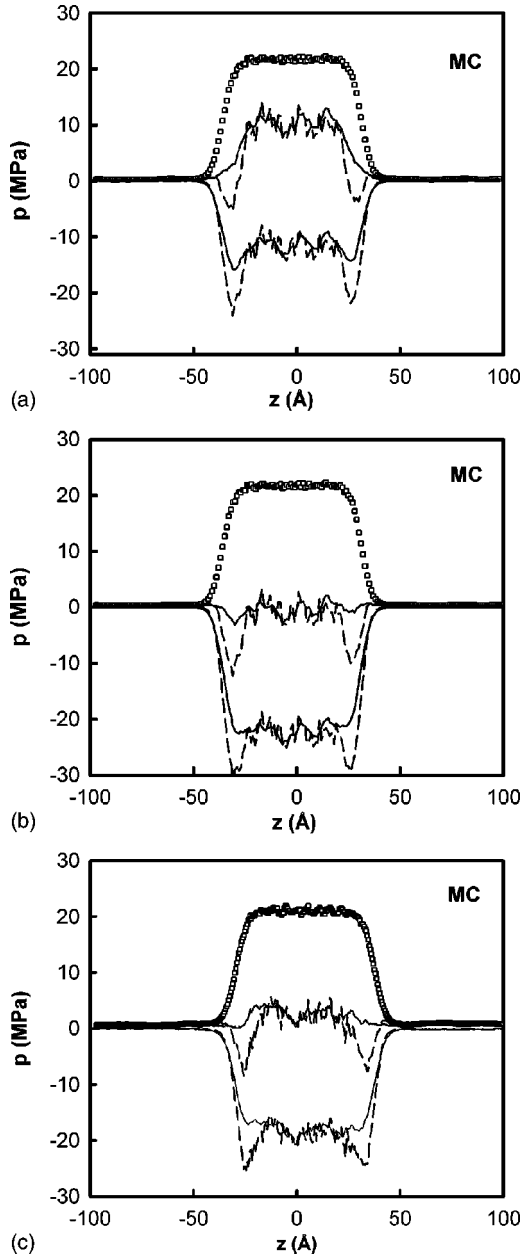

FIG. 3. (a) Normal and tangential pressure profiles calculated in MC using the u_T model without applying the long range corrections; (b) normal and tangential pressure profiles calculated in MC but using the f_{TC} force instead of the f_T in the calculation of the pressure tensor; c) components profiles calculated in MC using the u_{TS1} potential model. The upper curves represent the ideal gas contribution and/or the kinetic part whereas the lower curves represent the potential part of the pressure. The curves in the center of the parts (a), (b), and (c) of this figure correspond to the total pressure expressed as the sum of the ideal and potential parts.

components parts of the pressure tensor calculated over configurations resulting from MC simulations using a truncated u_T potential without any long range corrections. The profiles in Fig. 3(a) are obtained by using the f_T force in the calculation of the normal and tangential components of the pressure tensor. Interestingly, we see that the configurational part of the p_N and p_T components differ significantly for MC and MD methods whereas the difference in the profiles of the ideal term are caused by the different coexisting densities resulting from the two methods. In MC simulations, the local values of the normal and tangential components of the pressure are approximately the same in the vapor phase and in the liquid phase but differ between the two phases, indicating thus that apparently the configurations resulting from MC are not in mechanical equilibrium. In contrast to molecular dynamics method, Monte Carlo generates configurations by calculating the change in energy. The comparison between MC using a truncated potential and a MD using a truncated force is not really pertinent for a two phase system. Actually, the introduction of a cutoff leads to a discontinuity in both the potential energy and the force at r_c. At the cutoff distance, the force and the potential have a finite value which drops suddenly to zero just beyond the cutoff. It means that truncating the force at the cutoff leads to small impulses on atoms i and j when the distance r_{ij} exceeds r_c. To take into account this impulsive correction to the pressure tensor components, we follow the method already used by Trokhymchuk and Alejandre[13] which consists to add a δ function in the definition of the force as in Eq. (17),

$$f_{TC}(r_{ij}) = \begin{cases} -\dfrac{\partial u_{LJ}}{\partial r_{ij}} & r_{ij} < r_c \\ +\dfrac{u_{LJ}(r_c)}{\Delta r} & r_c < r_{ij} < r_c + \Delta r \\ 0 & r_{ij} \geqslant r_c + \Delta r \end{cases} \cdot \tag{17}$$

In Eq. (17) Δr is taken equal to 0.05 Å. Figure 3(b) presents the profiles of the normal and tangential components calculated with the f_{TC} force. The introduction of the $u_{LJ}(r_c)/\Delta r$ contribution between r_c and $r_c+\Delta r$ is sufficient to change significantly the profile of the potential part. In fact, the local values of the p_N and p_T components are now the same in the liquid phase and in the vapor phase. The normal component becomes constant throughout the interface. The configurations generated with MC using the u_T model are shown to be in mechanical equilibrium on condition that the f_{TC} force is used in the pressure tensor calculation. The part of the surface tension calculated from the virial expression is equal to $8.6\,\mathrm{mN\,m^{-1}}$ using the f_{TC} force whereas it is equal to 7.3 with f_T. As it can be seen in Fig. 3(b), the presence of this impulsive contribution to the pressure makes the peaks of the tangential part throughout the interface regions more negative in agreement with a higher value of the surface tension. In the work of Trokhymchuk and Alejandre,[13] it has been reported that MD using the f_T force corresponds to MC using the u_{TS1} model and MD with the f_{TC} corresponds to MC using the u_T potential. Our simulations also show that the best agreement between MC and MD using truncated potential and force is found between MC with u_{TS1} and MD with f_T. However, a more satisfactory agreement will not be obtained as long as the force is discontinuous at $r_{ij}=r_c$.

In fact, all the analytical forms of potentials we have used, up to now for this comparison, involve a discontinuity in their derivative with respect to r_{ij} at the cutoff distance and are not differentiable at the cutoff value.

To avoid a discontinuity of the derivative of the potential, we now add an additional term $(r_{ij}-r_c)(\partial u_{LJ}/\partial r_{ij})_{r_c}$ making thus the derivative of the potential zero at the cut off.

Downloaded 04 Jul 2008 to 194.214.132.32. Redistribution subject to AIP license or copyright; see http://jcp.aip.org/jcp/copyright.jsp

The potential and the force are expressed in Eq. (18) and in Eq. (19), respectively. A discontinuity remains in the derivative of the force, not in the force itself.

$$u_{TS2}(r_{ij}) = \begin{cases} u_{LJ}(r_{ij}) - u_{LJ}(r_c) - (r_{ij} - r_c)\left(\dfrac{\partial u_{LJ}}{\partial r_{ij}}\right)_{r_c} & r_{ij} < r_c \\ 0 & r_{ij} \geqslant r_c \end{cases}, \tag{18}$$

$$f_{TS}(r_{ij}) = \begin{cases} -\dfrac{\partial u_{LJ}}{\partial r_{ij}} + \left(\dfrac{\partial u_{LJ}}{\partial r_{ij}}\right)_{r_c} & r_{ij} < r_c \\ 0 & r_{ij} \geqslant r_c \end{cases}. \tag{19}$$

We show in Fig. 4(a) that MC using the u_{TS2} model and MD using the f_{TS} yield close density profiles leading to a deviation between the liquid densities of 2% (Table II). Figures 4(b) and 4(c) show that the profiles of the tangential and normal parts of the pressure tensor, calculated both in MC and MD, are similar within statistical fluctuations and that the configurations resulting from the two methods are in mechanical equilibrium. When shifted force or shifted potential are used to calculate surface tension, long range corrections to the surface tension must be included to account for both the long range interactions and the shift. Such long range corrections are approximate[45] and not easy to calculate. Consequently, we prefer to compare the surface tension values over the contribution calculated from the virial route in Eq. (11). The calculated values (Table II) can be considered as very close with the standard deviations. We conclude that the truncated and shifted potential u_{TS2} model and the truncated and shifted f_{TS} force do lead to the same point in the coexistence curve and that the mechanical and thermal equilibria are respected for MC and MD. We see that taking the derivative of the potential continuous at the cutoff radius is the key to yielding an agreement between both methods.

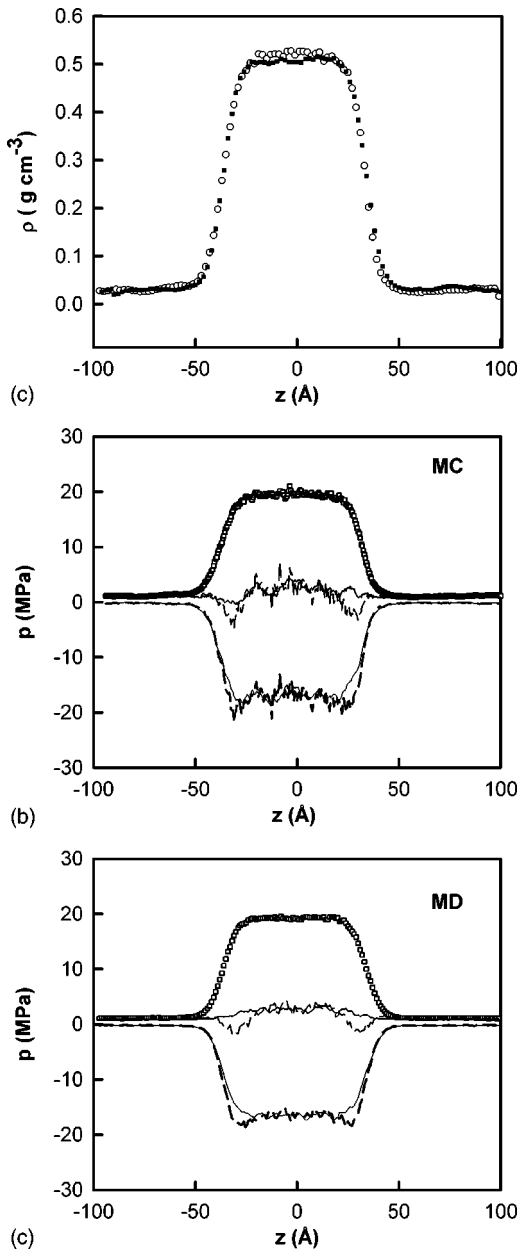

FIG. 4. (a) Density profiles at $T = 325$ K calculated in MC (○) using the u_{TS2} potential model and in MD (■) with the f_{TS} force; normal (——) and tangential (— — —) pressure profiles calculated in both (b) MC, and (c) MD.

C. MC and MD with models modified by switching functions

In order to avoid any problems concerning both the discontinuity in the potential and in the gradient of the force at the cutoff radius and the use of the long range corrections, we define consistent potential and force by taking the force and its derivative zero at the cutoff value. To do this, we use the Lennard–Jones potential $u_{LJ}(r_{ij})$, modified by a cubic spline[46–48] to give the following expressions for the potential and the force:

$$u_{SP}(r_{ij}) = \begin{cases} u_{LJ}(r_{ij}) - u_{LJ}(r_c) + a & r_{ij} < r_s \\ -\dfrac{b}{3}(r - r_c)^3 - \dfrac{c}{4}(r - r_c)^4 & r_s \leqslant r_{ij} < r_c, \\ 0 & r_{ij} \geqslant r_c \end{cases} \tag{20}$$

$$f_{SP}(r_{ij}) = \begin{cases} -\dfrac{\partial u_{LJ}}{\partial r_{ij}} & r_{ij} < r_s \\ +b(r - r_c)^2 + c(r - r_c)^3 & r_s \leqslant r_{ij} < r_c \\ 0 & r_{ij} \geqslant r_c \end{cases}. \tag{21}$$

The parameters a, b, and c are calculated by requiring that the first and second derivatives of the u_{SP} potential be continuous at r_s and r_c.

$$c = -\frac{\dfrac{\partial^2 u_{LJ}}{\partial r_{ij}^2}(r_c)}{(r_s - r_c)^2} + 2\frac{\dfrac{\partial u_{LJ}}{\partial r_{ij}}(r_c)}{(r_s - r_c)^3},$$

Downloaded 04 Jul 2008 to 194.214.132.32. Redistribution subject to AIP license or copyright; see http://jcp.aip.org/jcp/copyright.jsp

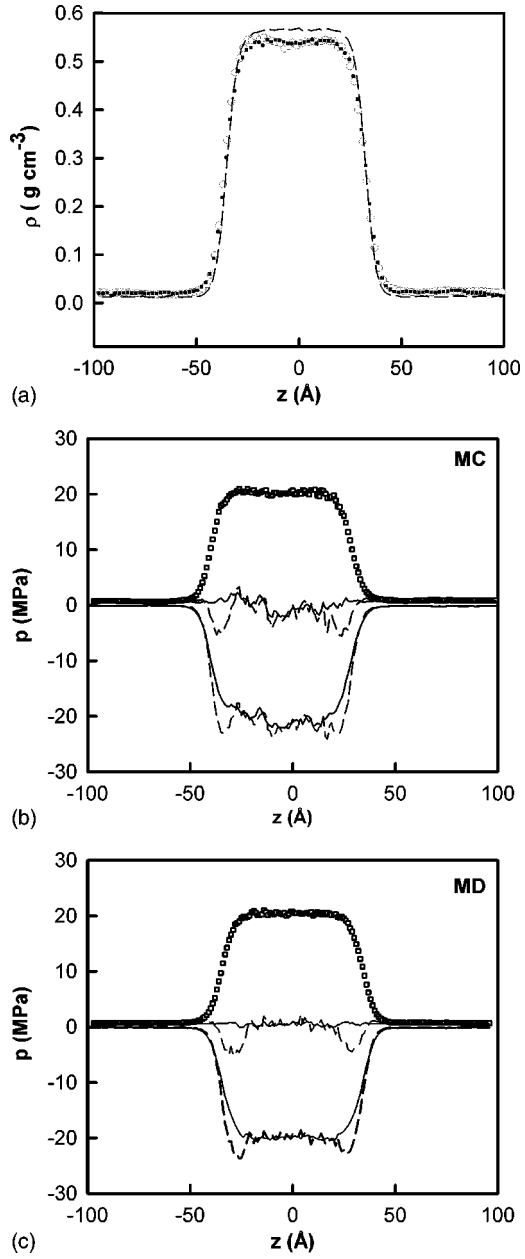

FIG. 5. (a) Density profiles at $T=325$ K calculated in MC (○) using the u_{SP} model and in MD (■) with the corresponding f_{SP} force. The dashed curve corresponds to the density profile calculated in MD using a cubic spline with a cutoff radius of 15 Å instead of 12 Å; normal (——) and tangential (— — —) pressure profiles calculated in both (b) MC and (c) MD.

$$b=\frac{\dfrac{\partial^2 u_{LJ}}{\partial r_{ij}^2}(r_c)}{(r_s-r_c)}-3\frac{\dfrac{\partial u_{LJ}}{\partial r_{ij}}(r_c)}{(r_s-r_c)^2}, \tag{22}$$

$$a=-\frac{b}{3}(r_s-r_c)^3-\frac{c}{4}(r_s-_c)^4.$$

MC simulation using the u_{SP} potential is compared with MD simulation using the f_{SP} force. We take the cutoff radius $r_c=12$ Å and $r_s=11$ Å. As expected, the density profiles, shown in Fig. 5(a), calculated from MC and MD simulations match very well. The liquid and vapor densities are identical within the statistical uncertainties (Table II). However, changing the potential function obviously amounts to significantly deviate the coexisting densities from the experimental values. The profiles of the tangential and normal components can be considered as similar for MC [Fig. 5(b)] and MD [Fig. 5(c)] within statistical fluctuations. We note that the oscillations of the pressure components calculated in the liquid phase are more marked in MC than in MD. From these pressure profiles, we may deduce the following equalities in the homogeneous phases $p_N^v=p_N^l=p_T^v=p_T^l$, where the superscripts v and l refer to the vapor and liquid phases, respectively. The configurations generated using both MC and MD are in mechanical equilibrium and correspond to the same point on the phase diagram. The surface tension values evaluated from the virial part are very close within the standard deviations calculated from the block averages. No truncation corrections must be added to the surface tension. As the long range contribution of the surface tension can reach up to 40% of the total value, it means that the surface tension calculated with a potential truncated via a cubic spline deviates very much from the experimental value. A calibration of this potential is thus required to predict accurate surface tension value and coexisting densities. We also observe that the increase in the cutoff radius ($r_c=15$ Å and $r_s=14$ Å) improves significantly the coexisting densities and the surface tension [Fig. 5(a), Table II]. However, the increase in the cutoff value makes the simulation with explicit interface cumbersome (keeping in mind that one of the initial objectives was to use a cutoff value of the order of that used in GEMC method). MC and MD lead to the same point in the phase envelope of the *n*-pentane under conditions that the force used in MD and in the calculation of the pressure tensor does not present any discontinuities at the cutoff radius. Taking the first derivative of the potential with respect to r_{ij} continuous is essential when we plan to simulate heterogeneous system; making thus the derivative of the force continuous allows to define a potential and force in a consistent manner.

An other important result we can extract from this study is that MD using standard force fields, which have been established from MC simulations, cannot predict accurately the phase diagram and the surface tension of *n*-alkanes. Using such force field, only MC calculations using a truncated potential can give accurate predictions for both the coexisting densities and surface tension when a rigorous calculation of the long range correction to the surface tension is applied. The implementation of the long range corrections to the configurational energy to the Metropolis scheme slightly increases the coexisting densities. It means that if we wish to make MC and MD consistent techniques for the prediction of the phase envelope of alkanes and for the use of long range corrections, one solution is to use a Lennard-Jones potential modified by a cubic spline. In this case, a new calibration is required and the development of new set of potential parameters is necessary, making inappropriate the present force fields of the literature.

D. Structural properties of the *n*-pentane chain

Concerning the conformation of the *n*-pentane, we calculate the profile along the direction normal to the interface

Downloaded 04 Jul 2008 to 194.214.132.32. Redistribution subject to AIP license or copyright; see http://jcp.aip.org/jcp/copyright.jsp

of the end-to-end distance of the molecule for MC and MD. These profiles are indistinguishable between MC and MD and do not depend on the truncation procedures. Further oscillations around the mean value are observed in the vapor phase. The mean value of the end-to-end distance calculated from the different slabs is 4.78 ± 0.03 Å for MC and 4.79 ± 0.03 Å for MD at $T = 299$ K. This same average distance decreases up to 4.72 ± 0.01 Å for MC and MD when the temperature is increased at 375 K. The comparison of the conformation shows that MC and MD lead to the same average structure of the *n*-pentane and to the same evolution of the structure as a function of temperature.

E. Dynamical properties of the liquid-vapor interface

To precisely investigate the sampling of the system along the *z* direction, we calculate the percentage of molecules which were found at least once inside the liquid and vapor phases over the 10 000 saved configurations. This percentage increases from 58% to 80% for MC and from 67% to 97% for MD as the temperature is increased from 299 K to 375 K. These percentages show that the sampling of the liquid-vapor system in the *z* direction is almost equally performed by MC and MD. The implementation of the algorithm allowing to use randomly two different magnitudes for the displacements makes the MC method competitive compared to MD for the moves of the molecules along the direction normal to the interface. One of the advantages of MD is the possibility of studying the dynamical properties at the interface, as for example, the residence time of pentane molecules in the interfacial region. The mean residence time is calculated from the correlation function $r(t)$ defined as[49,50]

$$r(t) = \frac{\langle P_j(t,t_i;t^*)\rangle_j}{\langle P_j(0,t_i;t^*)\rangle_j}, \tag{23}$$

where $P_j(t,t_i;t^*)$ is the Heaviside unit step function which is equal to 1 if the pentane molecule j lies within the interface region at both time t_i and $t_i + t$, and in the interim does not leave the interfacial zone for any continuous period longer than t^*. Otherwise, the unit step function is equal to zero. This function gives a probability for a pentane molecule to stay in the interface region during time t. The parameter t^* is introduced to take into account molecules which leave the interface temporarily, but for a time period shorter than t^*. The calculations are carried out using different values of t^* within the range 0.6–10 ps. The time correlation function $r(t)$ can be fitted to a second-order exponential decay:[51]

$$r(t) = A_1 \exp\left(-\frac{t}{\tau_1}\right) + A_2 \exp\left(-\frac{t}{\tau_2}\right). \tag{24}$$

In Eq. (24), the first term corresponds to an escape of the molecules located close to the border of the interface at a time about τ_1 ps. The second term describes a persistence of the molecules in the interface and τ_2 corresponds to the residence time of pentane molecules at the liquid-vapor interface. Roughly, the fitted parameters A_1 and A_2 can be interpreted as the percentage of molecules involved in both processes. We calculate the residence time of the molecules in the interface region by delimiting the interface region with two *z* positions. Each position is given within a fluctuation of ± 3 Å, which is taken into account in the calculation of $r(t)$. The residence time τ_2 in the interface region at T= 325 K increases from 22 ps to 46 ps as t^* is increasing from 0.6 ps to 10 ps. Although the choice of t^* is somewhat arbitrary, it can be seen that τ_2 is weakly dependent on the value of t^*. More exactly, between 0.6 ps and 2 ps, τ_2 is insensitive to the value of t^* whereas values of t^* varying from 2 to 20 ps affect significantly the residence time values. The $r(t)$ curves calculated using a value of t^* of 2 ps at the interface region are displayed in Figure 6 for $T = 325$ K and $T = 350$ K. This value of 2 ps has been already used in previous works[52,53] but with different systems. In addition, it is not clear that such a value of 2 ps is the most appropriated for the liquid-vapor interface system. Because of the dependence of t^* on T, it is difficult to extract a correlation between T and τ_2. When t^* is fixed to 2 ps, we find a value of τ_2 equal to 27 ps and 33 ps for $T = 325$ K and 350 K, respectively. It means that the variation of τ_2 with the temperature is much less marked than that of τ_2 with the parameter t^*. Less than 30% (A_1) of the pentane molecules are located close to the border to the interface and leave this zone at a time of about 3 ps (τ_1). This work represents the attempt to calculate the residence time of molecules at the interface region. A previous work has calculated the residence time of water molecule at the liquid-vapor interface and the authors have found a residence time of the order of 2 ps.[54] From the calculation of the residence time of *n*-pentane molecules, we can only say that the residence time in the interface region ranges roughly from 20 to 50 ps.

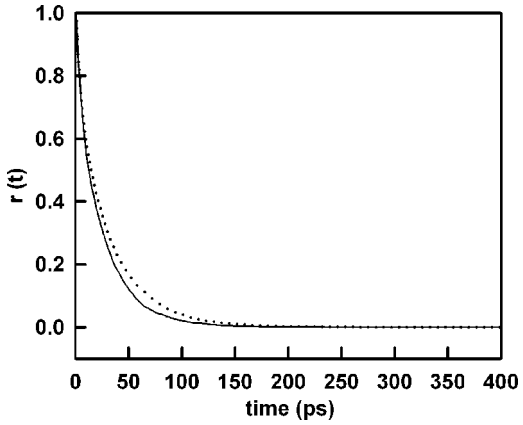

FIG. 6. Residence time correlation functions for the *n*-pentane molecule at the liquid-vapor interface region at $T = 325$ K (——) and $T = 350$ K (···).

IV. CONCLUSIONS

This work lies within the framework of direct molecular simulations of interfaces. As we have shown in the beginning of this paper, there is a great variety of direct simulations in the liquid-liquid and liquid-vapor interfaces, differing in their methodologies, energetic potential models (electrostatic contributions, polarization effects, and truncation procedures), and the technique used (MC and MD). This diversity results in important difficulties to discriminate between the different

Downloaded 04 Jul 2008 to 194.214.132.32. Redistribution subject to AIP license or copyright; see http://jcp.aip.org/jcp/copyright.jsp

contributions on the calculated properties. We have already established an efficient methodology for the determination of the coexistence properties and surface tension of the *n*-pentane using the MC approach.[23,24] When dealing with neutral molecules such as alkanes, we need not to take into account the way of describing the electrostatic and polarization contributions. Consideration must be only given to the way the nonbonded Lennard-Jones interactions are truncated. In addition, the study of the dynamical properties of the molecules at the interface region requires to make MC and MD results in agreement.

In this paper, we have performed various comparisons between MC and MD results on the basis of the values of coexisting densities and surface tension. We have shown that the MC simulations combining both the use of a truncated potential and the incorporation of the long range corrections to the configurational energy with the use of a moderate cutoff radius provide a good agreement between the calculated properties and the corresponding experimental values. Using force fields which have preliminary been established for alkanes from MC, it is expected that the direct MC calculations predicts much better than MD the phase coexistence density curve and the surface tension of alkanes. We have quantified the differences between the MD calculations using a truncated force and MC calculations using a truncated potential. This result is in line with what it was already observed in previous simulations involving MC and MD techniques of the LJ fluid liquid-vapor interface. These discrepancies are due to the fact that the potential function is not differentiable at the cutoff value, which therefore makes that the force in MD does not correspond to the potential in MC. However, we note that shifting the potential in MC improves the agreement with MD.

A satisfactory agreement between MC and MD can be obtained by using a shifted-force potential for which the derivative of the potential is continuous at the cutoff radius. To obtain a close agreement between MC and MD and avoid any long range interactions, we suggest changing the LJ potential by the addition of a polynomial function making thus the first derivative and second derivative of the potential continuous at the cutoff radius. We have demonstrated that the use of a such potential makes the MC and MD simulations identical concerning the density profiles and the pressure components profiles. However, the resulting coexisting densities and surface tension values present important deviations from experiments. One solution would be to increase considerably the cutoff radius but it does not correspond to an objective of computational efficiency. Another solution would consist in calibrating the LJ potential via a cubic spline and readjusting the potential parameters.

Concerning the structural properties of pentane, no difference has been found on the end-to-end distance between MC and MD and the potential models. In addition, we have shown that the two methods predict the same evolution of the end-to-end distance as a function of the temperature. One of our objectives was to calculate the residence time of the *n*-pentane molecules at the liquid-vapor interface. To do so, we have developed a specific algorithm and established a computational procedure. The residence time of the pentane molecules at the liquid-vapor interface ranges approximately from 20 ps to 50 ps.

ACKNOWLEDGMENTS

The authors want to acknowledge P. Ungerer for interesting discussions about this work and one of the authors (B.R.) would like to acknowledge the Institut du Développement et des Ressources en Informatique Scientifique (IDRIS) for a generous allocation of CPU time.

[1] M. Baaden, R. Schurhammer, and G. Wipff, J. Phys. Chem. B **106**, 434 (2002).
[2] B. Coupez, C. Boehme, and G. Wipff, J. Phys. Chem. B **107**, 9484 (2003).
[3] J. L. Rivera, C. McCabe, and P. T. Cummings, Phys. Rev. E **67**, 011603 (2003).
[4] L. X. Dang, J. Phys. Chem. B **103**, 8195 (1999).
[5] L. X. Dang, J. Phys. Chem. B **105**, 804 (2001).
[6] E. Salomons and M. Mareschal, J. Phys.: Condens. Matter **3**, 3645 (1991).
[7] E. Salomons and M. Mareschal, J. Phys.: Condens. Matter **3**, 9215 (1991).
[8] C. D. Holcomb, P. Clancy, and J. A. Zollweg, Fluid Phase Equilib. **75**, 185 (1992).
[9] C. D. Holcomb, P. Clancy, and J. A. Zollweg, Mol. Phys. **78**, 437 (1993).
[10] J. K. Johnson, J. A. Zollweg, and K. E. Gubbins, Mol. Phys. **78**, 591 (1993)
[11] M. Mecke, J. Winkelmann, and J. Fischer, J. Chem. Phys. **107**, 9264 (1997).
[12] M. Guo, D. Y. Peng, and B. C. Y. Lu, Fluid Phase Equilib. **130**, 19 (1997).
[13] A. Trokhymchuk and J. Alejandre, J. Chem. Phys. **111**, 8510 (1999).
[14] J. G. Powles, Physica A **126**, 289 (1984).
[15] A. Rosjorde, D. W. Fossmo, D. Bedeaux, D. Kjelstrup, and B. Hafskjold, J. Colloid Interface Sci. **232**, 1 (2000).
[16] A. Rosjorde, S. Kjelstrup, D. Bedeaux, and B. Hafskjold, J. Colloid Interface Sci. **240**, 355 (2001).
[17] J. G. Harris, J. Phys. Chem. **96**, 5077 (1992).
[18] L. A. N. Amaral and B. J. C. Cabral, J. Phys.: Condens. Matter **6**, 1919 (1993).
[19] G. A. Chapela, J. S. Rowlinson, and G. Saville, Faraday Discuss. Chem. Soc. **59**, 22 (1975).
[20] J. Alejandre, D. J. Tildesley, and G. A. Chapela, Mol. Phys. **85**, 651 (1995).
[21] J. M. Simon, S. Kjelstrup, D. Bedeaux, and B. Hafskjold, J. Phys. Chem. B **108**, 7186 (2004).
[22] A. Aguado, M. Wilson, and P. A. Madden, J. Chem. Phys. **115**, 8603 (2001).
[23] F. Goujon, P. Malfreyt, A. Boutin, and A. H. Fuchs, Mol. Simul. **27**, 99 (2001).
[24] F. Goujon, P. Malfreyt, A. Boutin, and A. H. Fuchs, J. Chem. Phys. **116**, 8106 (2002).
[25] M. Guo and B. C. Y. Lu, J. Chem. Phys. **106**, 3688 (1997).
[26] J. Lopez-Lemus and J. Alejandre, Mol. Phys. **100**, 2983 (2002).
[27] J. Lopez-Lemus and J. Alejandre, Mol. Phys. **101**, 743 (2003).
[28] P. Ungerer, C. Beauvais, J. Delhommelle, A. Boutin, B. Rousseau, and A. H. Fuchs, J. Chem. Phys. **112**, 5499 (2000).
[29] M. C. Martin and J. I. Siepmann, J. Phys. Chem. B **102**, 2569 (1998).
[30] W. L. Jorgensen, J. D. Madura, and C. J. Swenson, J. Am. Chem. Soc. **106**, 6638 (1984).
[31] B. Smit, S. Karaborni, and J. L. Siepmann, J. Chem. Phys. **102**, 2126 (1995).
[32] W. G. Hoover, Phys. Rev. A **31**, 1695 (1985).
[33] G. P. Morriss and D. J. Evans, Comput. Phys. Commun. **62**, 267 (1991).
[34] B. D. Butler, G. Ayton, O. G. Jepps, and D. J. Evans, J. Chem. Phys. **109**, 6519 (1998).
[35] G. Ayton, O. G. Jepps, and D. J. Evans, Mol. Phys. **96**, 915 (1998).
[36] O. G. Jepps, G. Ayton, and D. J. Evans, Phys. Rev. E **62**, 4757 (2000).
[37] J. P. R. B. Walton, D. J. Tildesley, and J. S. Rowlinson, Mol. Phys. **48**, 1357 (1983).
[38] J. P. R. B. Walton, D. J. Tildesley, and J. S. Rowlinson, Mol. Phys. **58**, 1013 (1986).
[39] B. D. Todd, P. J. Daivis, and D. J. Evans, Phys. Rev. E **51**, 4362 (1995).
[40] B. D. Todd, D. J. Evans, and P. J. Daivis, Phys. Rev. E **52**, 1627 (1995).
[41] J. G. Kirkwood and F. P. Buff, J. Chem. Phys. **17**, 338 (1949).

Downloaded 04 Jul 2008 to 194.214.132.32. Redistribution subject to AIP license or copyright; see http://jcp.aip.org/jcp/copyright.jsp

[42] J. Gmehling, CODATA Bull. **58**, 56 (1985).
[43] B. Smit and D. Frenkel, J. Chem. Phys. **94**, 5663 (1991).
[44] B. Smit, J. Chem. Phys. **96**, 8639 (1992).
[45] J. J. Nicolas, K. E. Gubbins, W. B. Street, and D. J. Tildesley, Mol. Phys. **37**, 1429 (1979).
[46] J. J. Erpenbeck, Phys. Rev. A **35**, 218 (1987).
[47] J. J. Erpenbeck, Phys. Rev. A **38**, 6255 (1988).
[48] B. L. Holian and D. J. Evans, J. Chem. Phys. **78**, 5147 (1983).
[49] S. H. Lee and J. C. Rasaiah, J. Chem. Phys. **101**, 6964 (1994).
[50] A. P. Lyubartsev and A. Laaksonen J. Phys. Chem. **100**, 16410 (1996).
[51] E. Hawlicka and D. Swiatla-Wojcik, Phys. Chem. Chem. Phys. **2**, 3175 (2000).
[52] D. E. Smith and L. X. Dang, J. Chem. Phys. **100**, 3757 (1994).
[53] R. Impey and L. X. Dang, J. Chem. Phys. **100**, 3757 (1994).
[54] R. S. Taylor, L. X. Dang, and B. C. Garrett, J. Phys. Chem. **100**, 11720 (1996).

Downloaded 04 Jul 2008 to 194.214.132.32. Redistribution subject to AIP license or copyright; see http://jcp.aip.org/jcp/copyright.jsp